ACS APPLIED MATERIALS & INTERFACES

Research Article

www.acsami.org

# Temperature-Dependent Wear Mechanisms for Magnetron-Sputtered AlTiTaN Hard Coatings

Vishal Khetan,[†,∥] Nathalie Valle,[†] David Duday,*[,†] Claude Michotte,[‡] Christian Mitterer,[§] Marie-Paule Delplancke-Ogletree,[∥] and Patrick Choquet[†]

[†]SAM Department, CRP-Gabriel Lippmann, 41, Rue du Brill, L-4422 Belvaux, Luxembourg

[‡]Ceratizit Luxembourg S.à.r.l., Route de Holzem, L-8232 Mamer, Luxembourg

[§]Department of Physical Metallurgy and Materials Testing, Montanuniversität Leoben, Franz-Josef-Strasse 18, A-8700 Leoben, Austria

[∥]Université Libre de Bruxelles, CP165/63, avenue F.D. Roosevelt 50, 1050 Bruxelles, Belgium

**ABSTRACT:** AlTiTaN coatings have been demonstrated to have high thermal stability at temperatures up to 900 °C. It has been speculated that the high oxidation resistance promotes an improved wear resistance, specifically for dry machining applications. This work reports on the influence of temperature up to 900 °C on the wear mechanisms of AlTiTaN hard coatings. DC magnetron-sputtered coatings were obtained from an $Al_{46}Ti_{42}Ta_{12}$ target, keeping the substrate bias at −100 V and the substrate temperature at 265 °C. The coatings exhibited a single-phase face-centered cubic AlTiTaN structure. The dry sliding tests revealed predominant abrasion and tribo-oxidation as wear mechanisms, depending on the wear debris formed. At room temperature, abrasion leading to surface polishing was observed. At 700 and 800 °C, slow tribo-oxidation and an amorphous oxide formed reduced the wear rate of the coating compared to room temperature. Further, an increase in temperature to 900 °C increased the wear rate significantly due to fast tribo-oxidation accompanied by grooving. The friction coefficient was found to decrease with temperature increasing from 700 to 900 °C due to the formation of oxide scales, which reduce adhesion of asperity contacts. A relationship between the oxidation and wear mechanisms was established using X-ray diffraction, Raman spectroscopy, scanning electron microscopy, surface profilometry, confocal microscopy, and dynamic secondary ion mass spectrometry.

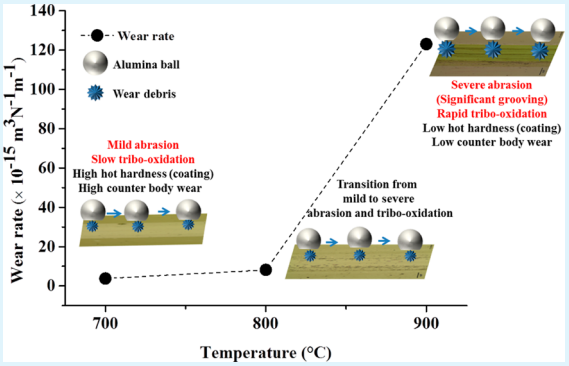


**KEYWORDS:** *TiAlN, wear mechanism, friction, hard coating, oxidation*

## 1. INTRODUCTION

Titanium aluminum nitride coatings have been of importance for the cutting tool industry for more than two decades.[1−3] These coatings enhance the performance of materials like cemented carbide and high speed steel used for making these tools.[3,4] Especially for applications up to 700 °C under dry conditions, they provide good oxidation and wear resistance.[4,5] However, for applications yielding higher temperature (≥800 °C) like dry high-speed machining, there is a need to further enhance the thermal and mechanical stability at these temperatures. Many strategies have been used to reach this objective. One such strategy is the addition of new elements such as Si, B, Ta, or Cr.[6−8] For example, Ta addition in TiAlN coatings enhances its oxidation resistance by limiting indiffusion of oxygen through its presence in the rutile lattice at temperatures up to 900 °C.[9]

Oxidation studies performed by Pfeiler et al. and Rachbauer et al. on AlTiTaN coatings deposited by cathodic arc evaporation and magnetron sputtering, respectively, have revealed that these coatings have much better oxidation resistance compared to TiAlN for temperatures up to 900 °C.[10,11] The oxidation mechanism of these coatings up to 950 °C was further studied by Khetan et al. for AlTiTaN coatings deposited using reactive magnetron sputtering.[12] Oxidation resistance along with properties like hot hardness, toughness, surface roughness, and thermal stability are important factors determining the wear resistance of a hard coating.[13] It can be expected that better oxidation resistance could enhance the wear resistance of the coating at high temperatures. Pfeiler et al.[9] investigated the wear performance of cathodic arc evaporated AlTiTaN coatings, which were found to be similar to TiAlN coatings in terms of wear resistance up to 700 °C. Wear investigation at 900 °C revealed complete coating failure for TiAlN, while the TiAlTaN coating survived the temperature but was worn out completely in the wear track under dry sliding conditions. Therefore, the enhanced oxidation resistance did

Received: June 19, 2014
Accepted: August 18, 2014
Published: August 18, 2014

  

not provide the expected wear resistance of AlTiTaN coatings at temperatures above 700 °C. Hence, there is a need to understand the wear mechanisms of these AlTiTaN coatings and their correlation with oxidation resistance at temperatures above 700 °C. Insight into the wear processes could aid later in the development of improved strategies of hard coatings concerning dry machining with working temperatures higher than 800 °C. Establishing a correlation between the oxidation and wear behavior of these coatings can facilitate this objective.

In this work, an attempt to correlate oxidation mechanisms and wear behavior of AlTiTaN coatings at temperatures from 700 up to 900 °C is made. The work identifies and elucidates the wear mechanisms using a combination of short and long duration ball-on-disc wear tests under dry sliding conditions within the temperature range of 700−900 °C. The resulting wear tracks were evaluated using surface profilometry, confocal optical microscopy, dynamic secondary ion mass spectrometry (D-SIMS), scanning electron microscopy (SEM), energy-dispersive X-ray spectroscopy (EDX), X-ray diffraction (XRD), and Raman spectroscopy techniques.

## 2. EXPERIMENTAL DETAILS

**2.1. Coating Deposition.** $Al_{0.48}Ti_{0.40}Ta_{0.12}N$ films were deposited in a homemade DC magnetron sputtering system. A 3-in.-diameter $Al_{46}Ti_{42}Ta_{12}$ target placed at an angle of 45° with respect to the substrate holder and at a distance of 9 cm was used, as described earlier.[12] The chamber was first pumped down to typically $3 \times 10^{-7}$ mbar; the substrate holder was preheated to 250 °C (at the end of the deposition time, a final temperature of 265 °C is reached); and then 5 sccm of Ar and 6 sccm of $N_2$ were injected, yielding a working pressure of 0.5 Pa. These flows were determined via a target poisoning study by investigating the variation of the target voltage as a function of the reactive gas flow, when the latter is the controlling variable to allow sputtering in the compound mode. The bias voltage was kept constant at −100 V.

The target was presputtered at 300 W (power density = 6.6 W/cm$^2$) for 10 min before deposition in order to decrease the amount of contaminants in the coatings. To ensure a uniform thickness of the coating, the substrate was rotated in the horizontal plane at 1.25 rpm. The coated substrates used for wear tests were $20 \times 7 \times 0.50$ mm$^3$ pieces of cemented carbide. The thicknesses and the deposition rate of the coatings were in the range of 3.0−3.5 $\mu$m and 0.8−1.0 $\mu$m/h, respectively. The as-deposited coatings exhibited a single-phase face-centered cubic structure with (111) preferred crystallographic orientation, evident in the XRD spectra.[12] The hardness of the coating was (33 ± 2) GPa, as reported earlier by the authors.[12] The elastic modulus was determined to be (415 ± 28) GPa, resulting in a nanohardness/elastic modulus ratio of 0.08.

**2.2. Tribological Tests.** The tribological behavior of the coatings was investigated by dry-sliding tests at room temperature (RT), 700, 800, and 900 °C on a CSM high-temperature ball on disc tribometer. The normal load, sliding speed, and radius of the wear track were kept constant at 2 N, 10 cm/s, and 7 mm, respectively. The load was kept at 2 N as it minimizes the chance of a sharp increase in flash temperature at the tribo-contact during wear test compared with 5 N used by different researchers[9] for similar coatings. Moreover, for a temperature of 900 °C, a load of 5 N is leading to a very rapid degradation of this kind of coating, inhibiting the comparison with lower temperature of wear. The 2 N load is the best compromise between sufficient coating lifetime and lack of friction measurement artifacts due to roughness of the samples. All tests were performed in ambient atmosphere against an alumina ball (Ø 6 mm). An alumina ball was used as a counter surface for its inertness to high temperature in ambient atmosphere. At room temperature, dry sliding tests were performed for 2500 laps (distance = 110 m). Two sets of wear measurements at temperatures of 700 up to 900 °C were made with different sliding distances. The first set included dry sliding tests performed for 5000 laps (distance = 220 m) at 700 and 800 °C. Within this set at 900 °C, the dry sliding test was performed only for 2500 laps (distance = 110 m). The reason for limiting the long duration tests at room temperature and 900 °C to 2500 laps was to retain a part of the AlTiTaN coating initially deposited.

In order to understand the influence of oxidation, an additional set of experiments consisting of short duration ball-on-disc tests (time: 7 min 19 s, laps: 1000, distance = 44 m) were performed at the same elevated temperatures: 700, 800, and 900 °C. The choice of this test duration was made to ensure a minimum wear debris generation, which could help to determine the origin of the wear process.

After the tribo-test, the wear scar on the alumina ball was observed using an optical microscope. This prompted easy evaluation of the wear rate in these conditions. The list of wear tests performed is summarized in Table 1.

**Table 1. List of Tribological Experiments Performed**

| temperature/laps | 1000 | 2500 | 5000 |
|---|---|---|---|
| 25 °C | na[a] | × | na[a] |
| 700 °C | × | na[a] | × |
| 800 °C | × | na[a] | × |
| 900 °C | × | × | na[a] |

[a]Not applicable.

**2.3. Characterization Techniques.** The chemical composition of the coatings was determined by EDX (error: 1.0 at. %) using a Hitachi SU 70 scanning electron microscope with an acceleration voltage of 20 keV. The surface imaging of the samples was performed in high-resolution mode with an accelerating voltage of 5 keV. Crystallographic investigations of as-deposited coatings were performed in the grazing incidence (GI) configuration (grazing angle = 2°) in a Bruker D8 Discover diffractometer using Cu K$\alpha$ radiation. Hardness measurements were carried out using a nanoindentation tester from CSM Instruments. Raman measurements were made using a Renishaw inVia Raman microscope. The spot size used for this measurement was ≤1 $\mu$m$^2$. The measurements were made using an excitation laser wavelength of 442 nm (He−Cd laser). The power used was 0.7 mW (wear tracks resulting from ball-on-disc tests at 700 and 800 °C) and 4 mW (wear track resulting from ball-on-disc test at 900 °C). Chemical depth profiling was carried out by D-SIMS in a CAMECA SC-Ultra instrument in positive ion mode, using $Cs^+$ ions with an impact energy of 1.0 keV. The total thicknesses of oxide layers were determined by combining the D-SIMS and surface profilometry techniques. A NanoFocus 3D confocal microscope $\mu$surf explorer was used for 3D imaging of the wear tracks.

## 3. RESULTS

**3.1. Wear Rate and Friction Behavior.** The two-dimensional depth profiles of the wear tracks after ball-on-disk tests were obtained for 5000 laps (700 and 800 °C) and 2500 laps (RT and 900 °C) (Figure 1a). Using the depth profiles, the wear rate of the AlTiTaN coating for different temperatures was evaluated. A decrease in wear rate from $(14 \pm 2) \times 10^{-15}$ m$^3$N$^{-1}$ m$^{-1}$ to $(3 \pm 0.5) \times 10^{-15}$ m$^3$ N$^{-1}$ m$^{-1}$ was observed when temperature is increased from room temperature to 700 °C. With an increase in temperature up to 800 °C, a slight increase in wear rate to $(6 \pm 2) \times 10^{-15}$ m$^3$ N$^{-1}$ m$^{-1}$ was observed. At 900 °C, the wear rate increased significantly to $(9 \pm 2) \times 10^{-14}$ m$^3$ N$^{-1}$m$^{-1}$, as shown in Figure 1b.

An initial increase in friction from 0.5 ± 0.1 to 0.8 ± 0.1 could be observed for increasing temperature as shown in Figure 1c. This can be due to removal of mild oxidative wear which results from removal of the thin oxide layer formed due to oxidation of the coating at 700 °C. The oxide formed is not wear resistant and increases the friction between the alumina

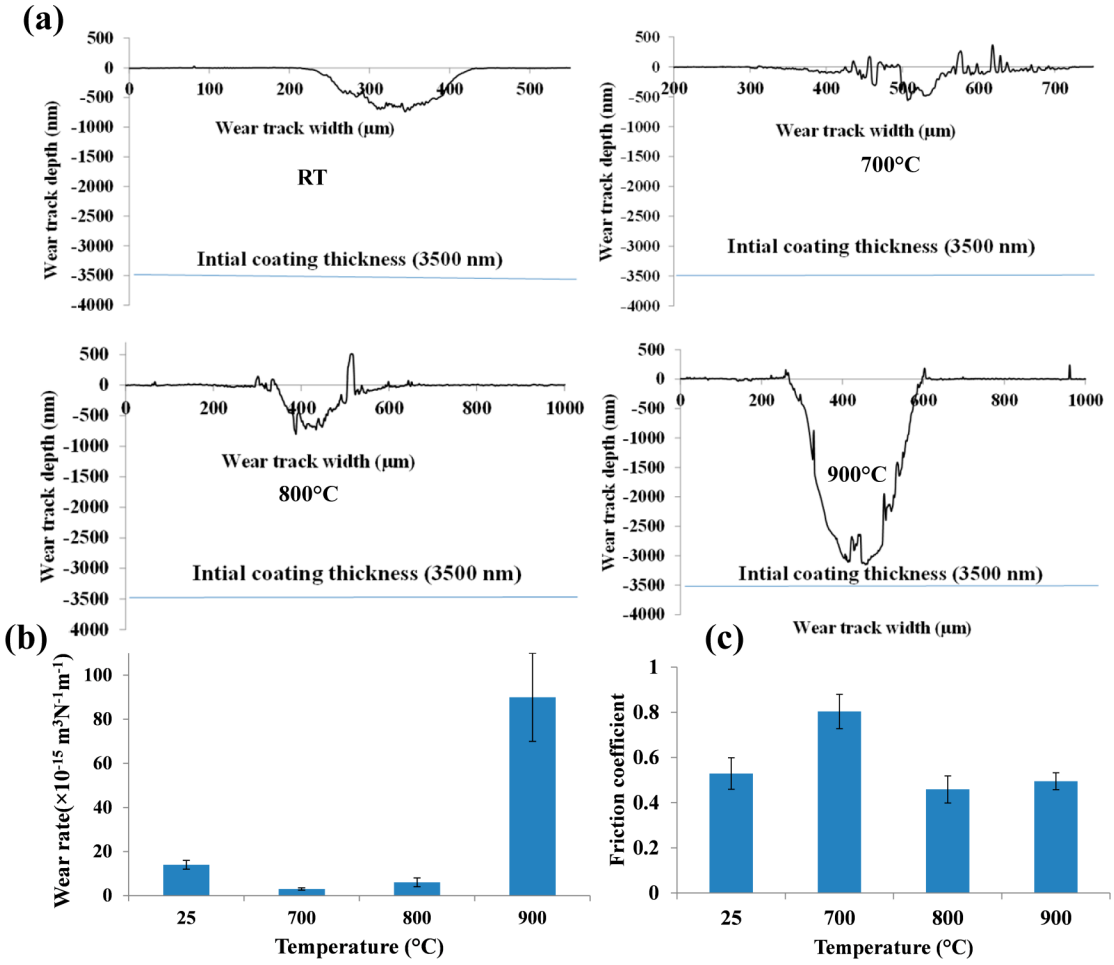


**Figure 1.** Comparison of (a) wear track depth profiles, (b) wear rate, and (c) average friction coefficient for the AlTiTaN coating after ball-on-disc wear tests performed at various temperatures for 2500 laps (RT and 900 °C) and 5000 laps (700 and 800 °C).

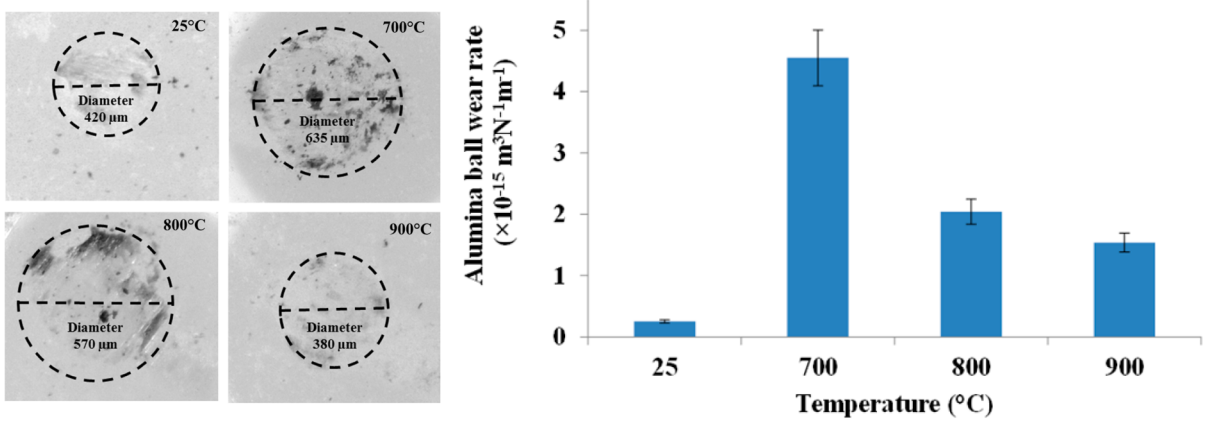


**Figure 2.** Optical microscope images of wear scars on the alumina balls and corresponding wear rate obtained after ball-on-disc tests at various temperatures performed for 2500 laps (RT and 900 °C) and 5000 laps (700° and 800 °C).

ball and the coating, leading to pronounced abrasion at 700 °C. Thicker oxide scales, which reduce adhesion of asperity contacts, lead to decreasing friction at 800 and 900 °C as shown in Figure 1c. This result is in agreement with previous studies performed on TiN, Cr−Al−V−N, and Ti−Al−V−N coatings[14−16] and $\alpha$-$Al_2O_3$.[17]

The wear scars observed on the alumina balls are displayed in Figure 2. The corresponding wear rates were calculated from the radius of the wear scar and are also given in Figure 2. The increase in the diameter of the wear scar on the alumina ball at 700 and 800 °C with respect to RT can in part be explained by the longer sliding distance used for these temperatures. However, since the wear rate is also increasing significantly, softening of the alumina balls at these temperatures is assumed to play a role. A thermally softened alumina ball in contact with an age-hardened[11] AlTiTaN coating surface with a very thin tribo-oxide can assist in easy removal of alumina from the ball surface. At even higher temperature, i.e., 900 °C, a possible


dx.doi.org/10.1021/am503942x | ACS Appl. Mater. Interfaces 2014, 6, 15403−15411

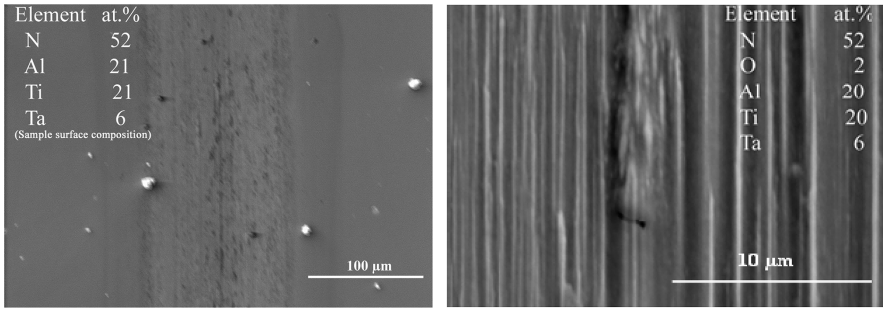


**Figure 3.** SEM micrograph of the wear track and corresponding EDX elemental composition for the pristine coating surface and the wear track obtained during a ball-on-disc test performed at room temperature. (Note: Error limit for metallic elements Al, Ti, and Ta is ±1 at. % and nonmetallic elements N and O is ±2 at. %.)

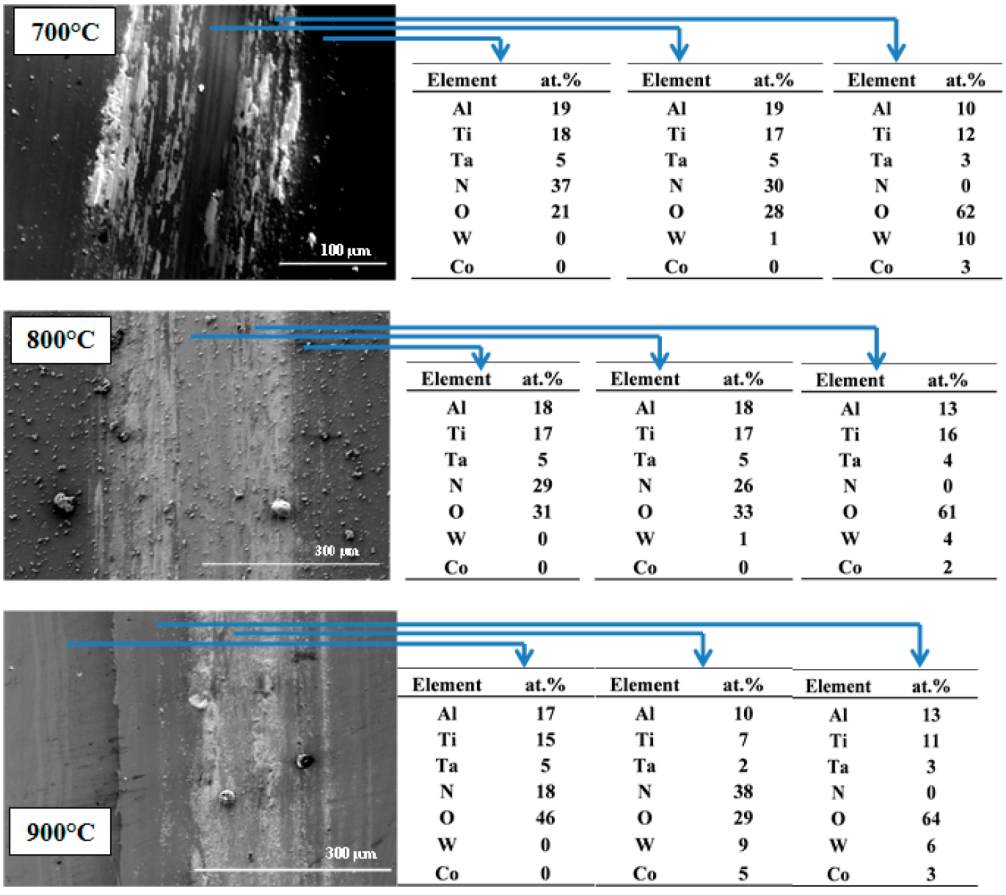


| Element | at.% | Element | at.% | Element | at.% |
|---|---|---|---|---|---|
| Al | 19 | Al | 19 | Al | 10 |
| Ti | 18 | Ti | 17 | Ti | 12 |
| Ta | 5 | Ta | 5 | Ta | 3 |
| N | 37 | N | 30 | N | 0 |
| O | 21 | O | 28 | O | 62 |
| W | 0 | W | 1 | W | 10 |
| Co | 0 | Co | 0 | Co | 3 |

| Element | at.% | Element | at.% | Element | at.% |
|---|---|---|---|---|---|
| Al | 18 | Al | 18 | Al | 13 |
| Ti | 17 | Ti | 17 | Ti | 16 |
| Ta | 5 | Ta | 5 | Ta | 4 |
| N | 29 | N | 26 | N | 0 |
| O | 31 | O | 33 | O | 61 |
| W | 0 | W | 1 | W | 4 |
| Co | 0 | Co | 0 | Co | 2 |

| Element | at.% | Element | at.% | Element | at.% |
|---|---|---|---|---|---|
| Al | 17 | Al | 10 | Al | 13 |
| Ti | 15 | Ti | 7 | Ti | 11 |
| Ta | 5 | Ta | 2 | Ta | 3 |
| N | 18 | N | 38 | N | 0 |
| O | 46 | O | 29 | O | 64 |
| W | 0 | W | 9 | W | 6 |
| Co | 0 | Co | 5 | Co | 3 |

**Figure 4.** SEM micrographs and EDX elemental compositions of the wear tracks formed during ball-on-disc tests performed at various temperatures. (Note: Error limit for metallic elements Al, Ti, Ta, W, and Co is ±1 at. %, and nonmetallic elements N and O is ±2 at. %.)

decrease in hot hardness of the over-aged coating[11] and/or a higher fraction of softened oxide scale on the coating surface could lead to the decreasing ball wear.

In the next sections, the wear behavior obtained for the AlTiTaN coatings at all temperatures will be evaluated individually.

**3.2. Tribological Behavior at Room Temperature.** A SEM overview of the wear track and the corresponding zoomed detail of the wear track are displayed in Figure 3. Grooves with width in the range 0.5−1.0 $\mu$m could be observed within the wear track. This observation suggests the wear mechanism is abrasion, leading to surface polishing. Further, the presence of moisture or $O_2$ in the tribological contact contributes to wear at room temperature in ambient air. The presence of oxygen (2 at. %), as detected by EDX analyses on the wear track, compared to those done at the pristine surface (see Figure 3) further supports this hypothesis. Tribochemical reactions between the coating and $O_2$ and/or moisture in the environment determine the wear behavior as explained by Pfeiler et al.[9]

**3.3. Tribological Behavior at 700° and 800 °C.** At both temperatures, the wear rate was lower than at room temperature (Figure 1b). The wear rate at 800 °C was slightly higher than at 700 °C which could be due to a more pronounced tribo-oxidation rate at 800 °C. SEM micrographs obtained on these two wear tracks (Figure 4) show the presence of abrasion and tribo-oxidation as the dominant wear mechanism controlling the wear at 700 and 800 °C. Wear tests at these temperatures revealed that the nature of the oxide

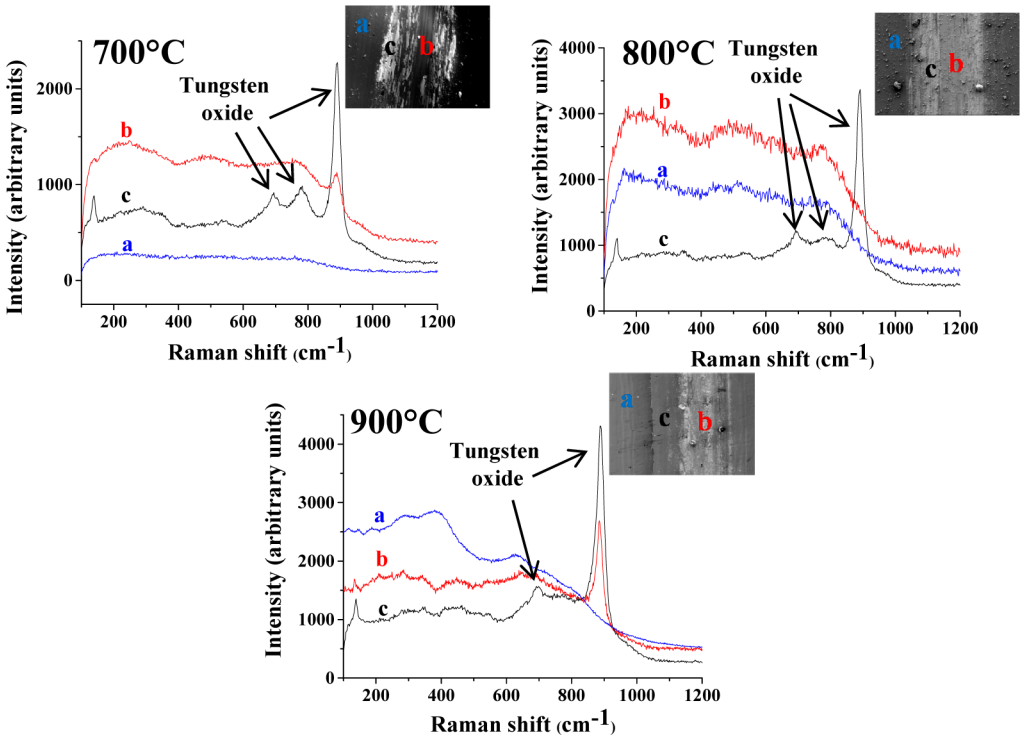


**Figure 5.** Raman spectra of the wear tracks formed during ball-on-disc tests performed at various temperatures for 2500 laps (900 °C) and 5000 laps (700 and 800 °C): (a) pristine sample surface, (b) center of wear track, and (c) border of wear track.

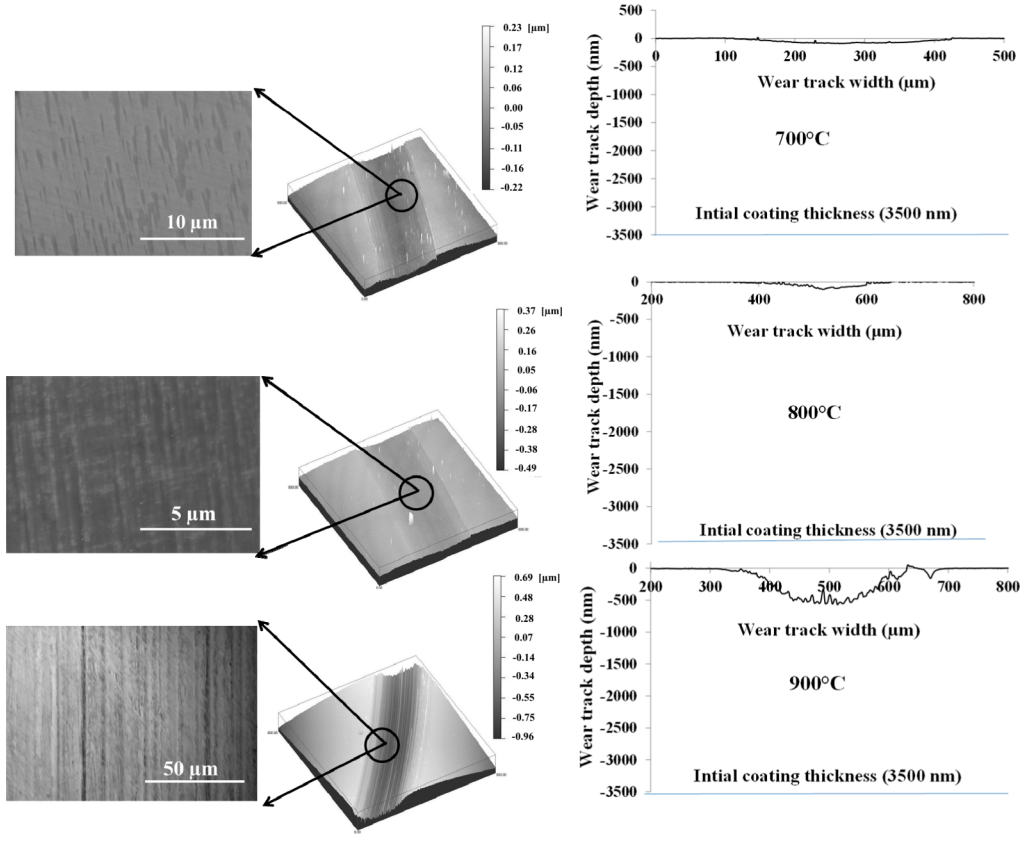


**Figure 6.** Confocal microscopy images with corresponding zoomed SEM view of wear tracks obtained after ball-on-disc tests at 700, 800, and 900 °C performed for 1000 laps.

formed and the rate of tribo-oxidation control the wear behavior of the coating. The film essentially contains oxide scales containing Ti, Al, and Ta, which was supported by EDX analysis (Figure 4). W-oxides are present very locally, due to


dx.doi.org/10.1021/am503942x | ACS Appl. Mater. Interfaces 2014, 6, 15403−15411

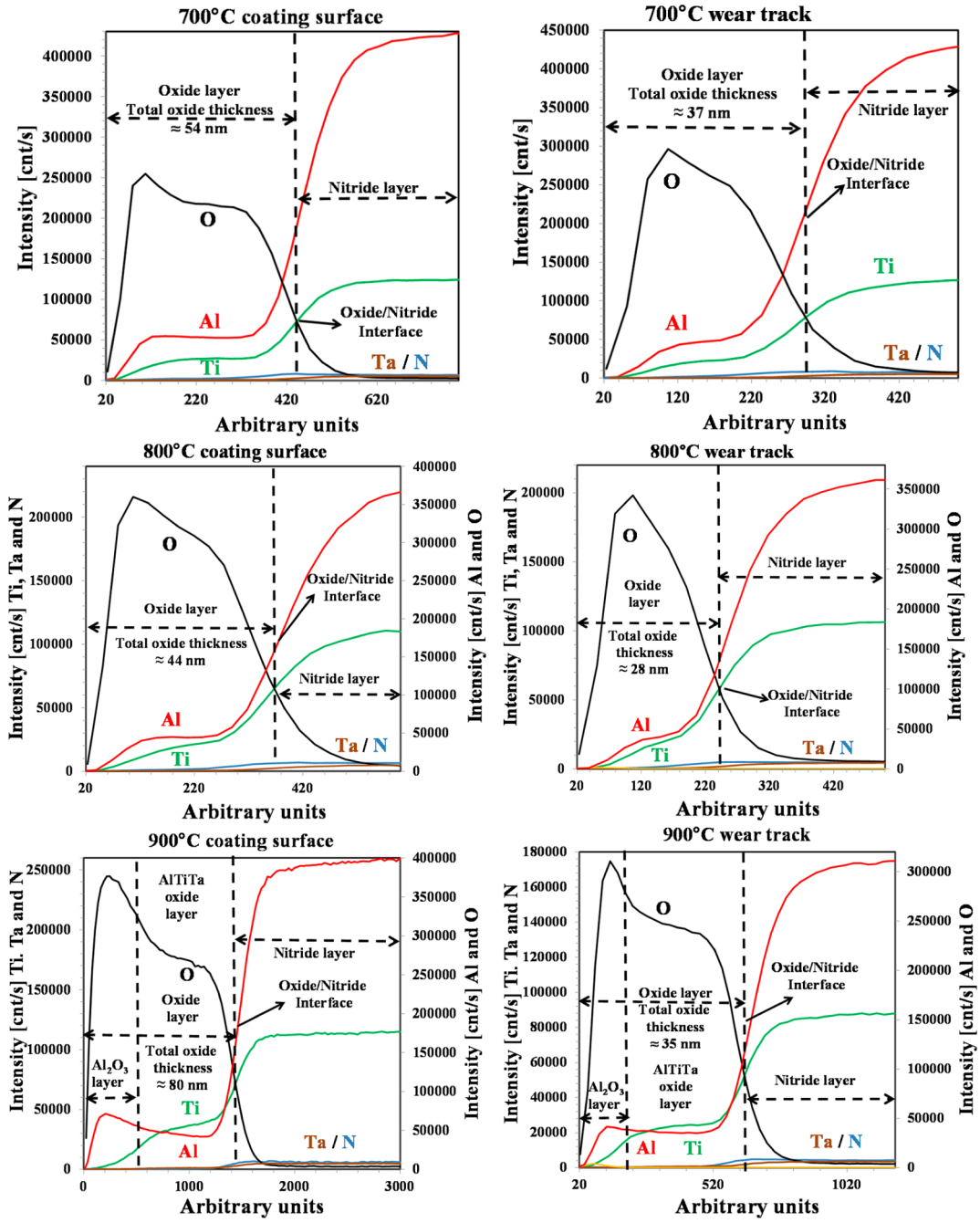


**Figure 7.** D-SIMS depth profiles for coating surface and wear tracks obtained after ball-on-disc tests at 700, 800, and 900 °C performed for 1000 laps.

oxidation and sublimation of reaction products from the uncoated local part of the cemented carbide substrate. They could also appear due to the presence of some defects at the surface of the coating. When these defects are removed from the surface, the cemented carbide substrate can be very locally oxidized, and the corresponding oxide can pollute the wear track surface.

Raman spectroscopy was performed in the wear track and on the pristine sample surface to further understand the nature of oxides present in the wear track. As shown in Figure 5, no significant peak or band could be observed on the pristine coating surface. This indicated the presence of a Raman-inactive coating material or an amorphous layer on top of the oxidized coating from which no significant signal could be obtained. The above observation is in agreement with the presence of an amorphous oxide layer formed when the AlTiTaN coating is air-annealed at 700 °C.[12] At 800 °C, the obtained very broad bands are possibly corresponding to either the $Ti_{1-x}Al_xN$ (273 and 651 $cm^{-1}$) or the $TiO_2$ (rutile) phase (565 and 641 $cm^{-1}$).[18] Since broad bands are observed in the Raman spectra, they indicate that the phase present is poorly crystalline or contains a large number of defects. With respect to the two different zones observed in the wear track, Raman spectroscopy supported the SEM observation for both temperatures. The Raman spectra obtained in the center (area b) of the wear track obtained at 700 °C (Figure 5) displayed only broad Raman bands and one peak corresponding to tungsten oxide at 891 $cm^{-1}$, indicating the presence of a


dx.doi.org/10.1021/am503942x | ACS Appl. Mater. Interfaces 2014, 6, 15403−15411

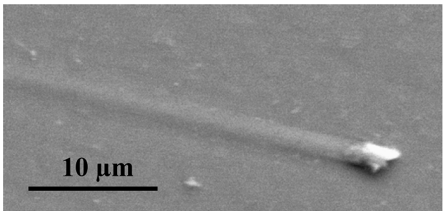


| Element/Location | Wear track (at.%) | Wear debris (at.%) |
|---|---|---|
| N | 44 | 12 |
| O | 11 | 47 |
| Al | 19 | 15 |
| Ti | 20 | 13 |
| Ta | 6 | 3 |

**Figure 8.** SEM image and corresponding EDX chemical composition of groove-forming wear particles obtained after a ball-on-disc test at 800 °C for 1000 laps.

complex (containing Ti, Al, and Ta) polycrystalline oxide and a small fraction of tungsten oxide.[18] A similar Raman signal was observed in the edge of the wear track (area c) displaying peaks at 111, 696, 833, and 891 $cm^{-1}$, indicating the presence of tungsten oxide particles in the wear track. This confirms a higher sublimation rate or the agglomeration of W-oxide debris at the border of the wear track. For 800 °C, the Raman spectra of both the areas studied in the wear track are similar to those observed at 700 °C, which suggests similar wear behavior of the AlTiTaN coatings at these temperatures.

**3.4. Tribological Behavior at 900 °C.** At 900 °C, the highest coating wear rate compared to all other temperatures investigated was observed. This high wear rate could be attributed to the consequently high rate of tribo-oxidation at this temperature. It could be further enhanced through possible overaging and thus softening of the coating.[11,19] Additionally, the crystalline nature of the oxide formed, which is promoted at this temperature (which is harder than its amorphous form),[20] could also contribute to the increase in wear rate.

Raman spectroscopy was performed in the wear track after the test at this temperature as shown in Figure 5. The Raman spectra on the sample surface (area a) clearly revealed the presence of broad bands corresponding to $Ti_{1-x}Al_xN$ (273 $cm^{-1}$) and rutile (453 and 641 $cm^{-1}$).[18] This indicates faster crystallization of the rutile phase at 900 °C compared to wear tests performed at 700 and 800 °C. The presence of tungsten oxide within the wear track was confirmed with peaks observed at 111, 696, 833, and 891 $cm^{-1}$ (Figure 5). SEM and EDX examinations (Figure 4) also support this observation.

**3.5. Short Duration Tests.** After short duration tests, the resulting wear tracks (two-dimensional view, three-dimensional view, and corresponding SEM micrographs, corresponding D-SIMS depth profiles) display mild abrasion with tribo-oxidation at 700 °C (Figure 6 and Figure 7). With an increase of the temperature to 800 °C, a slightly severe form of abrasive wear,[21] i.e., grooving within the wear track, could be observed (groove width: ~ 2.5 μm), as displayed in Figure 6. Grooving becomes prominent at 900 °C (groove width: 7−9 μm) and leads to more pronounced abrasive wear as shown in Figure 6. The three-dimensional confocal microscopy images obtained for the 700 and 800 °C wear tracks show the presence of outgrowing oxides scattered on the surface, which could be associated with an oxide debris growth mechanism when they are trapped and agglomerated in the wear track. Consequently, it can be proposed that the detachment of these outward growing oxides can be at the origin of wear particles observed in the wear tracks, leading to the grooving mechanism (Figure 8).

For each of the high-temperature ball-on-disk tests, D-SIMS measurements were carried out on the coating surface and within the wear track to understand the nature of the oxides formed (tribo-film and oxide formed during the last few seconds of the wear test) responsible for the wear behavior at individual temperatures. It must be stated that oxidation during cooling after the wear test did take place. This brings in a slight overestimate of the oxide thickness under consideration, but this does not influence the nature of oxide formed at different temperatures, which can have an impact on different modes of wear.

At 700 and 800 °C, the formation of a single oxide layer (uniform distribution of Al, Ti, and Ta) within the tribo-film (including the oxidation during cooling after the wear test) has been observed, as displayed in Figure 7. A slight enrichment of Al was observed in the oxide scale formed on the surface far away from the wear track at 800 °C. At 900 °C, the tribo-film displayed a bilayer oxide comprised of an $Al_2O_3$ layer on top and a mixed AlTiTa oxide layer at the nitride layer (Figure 7). The observations were in agreement with the results of oxidation experiments performed by Khetan et al., which described the change from an amorphous oxide monolayer at 700 °C to a crystalline bilayer oxide at 900 °C.[12]

## 4. DISCUSSION

The goal of this work is to establish a correlation between oxidation and wear mechanisms of AlTiTaN coatings at different temperatures. The observations in this study demonstrate that depending on the temperature the possible wear mechanisms can be classified as abrasion and surface polishing at room temperature, abrasion and slight oxidation at 700 °C with an increase of these phenomena at 800 °C, and rapid abrasion with higher oxidation kinetics at 900 °C.

Compared to all other temperatures investigated in this study, a rapid increase in wear rate at 900 °C has been observed. This can be due to two factors: (a) a decrease in hot hardness of the coating when the temperature reaches 900 °C[11,19] or/and (b) an increase in the oxidation rate as described by Khetan et al.[12] of the coating, generating more oxide which is soft and easy to remove after each lap. Supporting evidence of high oxidation rate in this study comes from D-SIMS profiles, which show a much thicker oxide developed on the coating surface (i.e., away from the wear track) at 900 °C (80 nm) compared to temperatures at or below 800° (44 nm) (Figure 7) for the same oxidation time.

Another important observation made through SEM and confocal microscopy (Figure 6) was the presence of grooving within the wear track for all tested temperatures. Grooving is well-known in the literature as a severe abrasive wear mode compared to other modes of abrasive wear.[21] An example of a compacted wear particle, which results in grooving, has been presented using SEM imaging for an AlTiTaN coating, tribo-tested at 800 °C for 1000 laps (Figure 8). Generation of these wear particles could stem from the formation of outgrowing oxides, which fail under the tribological load and can form oxide wear debris by accumulation. The presence of these

outgrowing oxides can result in high compressive stress developed during the oxidation process. This is due to a large molar volume difference between nitride and oxide as described by McIntyre et al. for TiAlN coatings.[22] The generation of these outgrowing oxides, which form the groove-forming wear particles, depends on the oxidation rate, and consequently, the density increases with the temperature. According to our observations, this phenomenon can be considered as very critical at 900 °C. The disintegrated oxide originating from both counter body alumina (which can soften at temperatures >700 °C) and AlTiTaN coating can promote greater abrasion of the coating at the tribo-contact through formation of compacted oxide/wear particles leading to a rapid increase in wear rate at 900 °C compared to 700 and 800 °C. This phenomenon has been observed by Stott et al.[23] who examined the role of oxidation on the formation of tribo-films on the surface and demonstrated development of compacted oxides.

The D-SIMS studies show that there are thinner oxides in the wear track compared to the sample surface exposed for oxidation (Figure 7) at all temperatures investigated. This result was expected as oxide is continuously being removed at the tribo-interface during the test. Another interesting observation given by D-SIMS is the comparison of the elemental distributions for the different constituent elements (Al, Ti, Ta, O, and N) present in the wear track and at the unworn oxidized coating surface. The elemental depth profiles are similar for the wear track and the unworn coating surface. On the basis of the conclusions of earlier work done on the same AlTiTaN coatings by the authors,[12] where they have shown that the oxide layers developed at 700, 800, and 900 °C are distinct and characteristic of the respective temperatures, it can be suggested from this D-SIMS analysis that the tribological flash temperature (i.e., the local temperature peaks occurring at asperities in contact)[24−26] is only slightly higher than the original test temperatures and not higher than 50 °C, according to the differences seen in the D-SIMS depth profiles shown in Figure 7 for the unworn coatings and the wear tracks.

## 5. CONCLUSIONS

AlTiTaN hard coatings were deposited on cemented carbide substrates with a face-centered cubic structure using DC magnetron sputtering, and their performance during wear tests at various temperatures was evaluated. The obtained results have shown that the wear mechanism of $Al_{0.48}Ti_{0.40}Ta_{0.12}N$ coatings at temperatures higher than or equal to 700 °C is dependent on the type and on the thickness of oxide formed and the softening of the coating under hot conditions during the wear test. The most prominent mode of wear at all temperatures is abrasion, which is controlled by the oxidation kinetics and by groove formation. These groove formations result from wear debris formed at the tribo-interface and generated from the outgrowing oxide which disintegrates from the nitride layer during the ball-on-disk test. At 700 and 800 °C, slow tribo-oxidation is measured and is associated with the formation of an amorphous/poorly crystalline oxide layer which can reduce the wear rate compared to room temperature. At 900 °C, a possible reduction of coating's hardness combined with enhanced tribo-oxidation and severe abrasion through dominant groove formation promotes high wear.

## AUTHOR INFORMATION

### Corresponding Author

*E-mail: duday@lippmann.lu.

### Author Contributions

All authors have given approval to the final version of the manuscript.

### Notes

The authors declare no competing financial interest.

## ACKNOWLEDGMENTS

The financial support by the National Research Fund (FNR, Luxembourg) under the frame of the SpiTriCoat project is gratefully acknowledged. Valuable time provided by Dr. Remi Aninat for SEM investigations and support provided by B. El Adib for making D-SIMS characterizations are appreciated. We also thank Dr. Mael Guennou and Mr. Mads Weber for making Raman spectroscopy measurements and helping in their interpretation.

## REFERENCES

(1) Mayrhofer, P. H.; Mitterer, C.; Hultman, L.; Clemens, H. Microstructural Design of Hard Coatings. *Prog. Mater. Sci.* **2006**, *51*, 1032−1114.

(2) PalDey, S.; Deevi, S. C. Single Layer and Multilayer Wear Resistant Coatings of (Ti,Al)N: a Review. *Mater. Sci. Eng., A* **2003**, *342*, 58−79.

(3) Mo, J. L.; Zhu, M. H.; Lei, B.; Leng, Y. X.; Huang, N. Comparison of Tribological Behaviours of AlCrN and TiAlN Coatings-Deposited by Physical Vapor Deposition. *Wear* **2007**, *263*, 1423−1429.

(4) Wang, D. Y.; Chang, C. L.; Wong, K. W.; Li, Y. W.; Ho, W. Y. Improvement of the Interfacial Integrity of (Ti,Al)N Hard Coatings Deposited on High Speed Steel Cutting Tools. *Surf. Coat. Technol.* **1999**, *120−121*, 388−394.

(5) Zhou, Z.; Rainforth, W. M.; Luo, Q.; Hovsepian, P. Eh.; Ojeda, J. J.; Romero-Gonzalez, M. E. Wear and Friction of TiAlN/VN Coatings Against $Al_2O_3$ in Air at Room and Elevated Temperatures. *Acta Mater.* **2010**, *58*, 2912−2925.

(6) Fuentes, G. G.; Almandoz, E.; Pierrugues, R.; Martínez, R.; Rodríguez, R. J.; Caro, J.; Vilaseca, M. High Temperature Tribological Characterisation of TiAlSiN Coatings Produced by Cathodic Arc Evaporation. *Surf. Coat. Technol.* **2010**, *205*, 1368−1373.

(7) Kathrein, M.; Michotte, C.; Penoy, M.; Polcik, P.; Mitterer, C. Multifunctional Multi-component PVD Coatings for Cutting Tools. *Surf. Coat. Technol.* **2005**, *200*, 1867−1871.

(8) Fox-Rabinovich, G. S.; Kovalev, A. I.; Aguirre, M. H.; Beake, B. D.; Yamamoto, K.; Veldhuis, S. C.; Endrino, J. L.; Wainstein, D. L.; Rashkovskiy, A. Y. Design and Performance of AlTiN and TiAlCrN PVD Coatings for Machining of Hard to Cut Materials. *Surf. Coat. Technol.* **2009**, *204*, 489−496.

(9) Pfeiler, M.; Fontalvo, G. A.; Wagner, J.; Kutschej, K.; Penoy, M.; Michotte, C.; Mitterer, C.; Kathrein, M. Arc Evapouration of Ti-Al-Ta-N Coatings: The Effect of Bias Voltage and Ta on High-Temperature Tribological Properties. *Tribol. Lett.* **2008**, *30*, 91−97.

(10) Pfeiler, M.; Scheu, C.; Hutter, H.; Schnöller, J.; Michotte, C.; Mitterer, C.; Kathrein, M. On the Effect of Ta on Improved Oxidation Resistance of Ti−Al−Ta−N Coatings. *J. Vac. Sci. Technol., A* **2009**, *7*, 554−560.

(11) Rachbauer, R.; Holec, D.; Mayrhofer, P. H. Increased Thermal Stability of Ti−Al−N Thin Films by Ta Alloying. *Surf. Coat. Technol.* **2012**, *211*, 98−103.

(12) Khetan, V.; Valle, N.; Duday, D.; Michotte, C.; Delplancke, M. P.; Choquet, P. Influence of Temperature on Oxidation Mechanisms of Fiber-Textured AlTiTaN Coatings. *ACS Appl. Mater. Interfaces* **2014**, *6*, 4115−4125.

(13) Findik, F. Latest Progress on Tribological Properties of Industrial Materials. *Mater. Des.* **2014**, *57*, 218−244.

(14) Fateh, N.; Fontalvo, G. A.; Gassner, G.; Mitterer, C. Influence of High-Temperature Oxide Formation on the Tribological Behaviour of TiN and VN Coatings. *Wear* **2007**, *262*, 1152−1158.

(15) Franz, R.; Neidhardt, J.; Sartory, B.; Kaindl, R.; Tessadri, R.; Polcik, P.; Derflinger, V. H.; Mitterer, C. High-Temperature Low-Friction Properties of Vanadium-Alloyed AlCrN Coatings. *Tribol. Lett.* **2006**, *23*, 101−107.
(16) Pfeiler, K.; Kutschej, K.; Penoy, M.; Michotte, C.; Mitterer, C.; Kathrein, M. The Effect of Increasing V Content on Structure, Mechanical and Tribological Properties of Arc Evaporated Ti−Al−V−N Coatings. *Int. J. Refract. Met. Hard Mater.* **2009**, *27*, 502−506.
(17) Schalk, N.; Mitterer, C.; Czettl, C.; Sartory, B.; Penoy, M.; Michotte, C. Dry-Blasting of $\alpha$- and $\kappa$-$Al_2O_3$ CVD Hard Coatings: Friction Behaviour and Thermal Stress Relaxation. *Tribol. Lett.* **2013**, *52*, 147−154.
(18) Karim, N. J.; Ben-Amotz, D. Chemical Imaging of Tribological Nitride Coated (TiN, TiAlN) Surfaces. *Wear* **2002**, *252*, 956−969.
(19) Mayrhofer, P. H.; Hörling, A.; Karlsson, L.; Sjölén, J.; Larsson, T.; Mitterer, C.; Hultman, L. Self-Organized Nanostructures in the Ti−Al−N System. *Appl. Phys. Lett.* **2003**, *83*, 2049−2051.
(20) Szczyrbowski, J.; Bräuer, G.; Ruske, M.; Bartella, J.; Schroeder, J.; Zmelty, A. Some Properties of $TiO_2$ Layers Prepared by Medium Frequency Reactive Sputtering. *Surf. Coat. Technol.* **1999**, *112*, 261−266.
(21) Stachowiak, W. W.; Batchelor, A. W. *Engineering Tribology*, 3rd ed.; Elsevier: New York, 2006.
(22) McIntyre, D.; Greene, J. E.; Hakansson, G.; Sundgren, J.-E.; Münz, W.-D. Oxidation of Metastable Single Phase Polycrystalline Ti0.5Al0.5N Films: Kinetics and Mechanisms. *J. Appl. Phys.* **1990**, *67*, 1542−1553.
(23) Stott, F. H.; Wood, G. C. The Influence of Oxides on the Friction and Wear of Alloys. *Tribol. Int.* **1978**, *11*, 211−218.
(24) Bowden, F. P.; Tabor, D. *The Friction and Lubrication of Solids*; Clarendon Press: Oxford, 1950.
(25) Archard, J. F. The Temperature of Rubbing Surfaces. *Wear* **1959**, *2*, 438−455.
(26) Blok, H. The Flash Temperature Concept. *Wear* **1963**, *6*, 483−494.